DALTON
FULL PAPER

Tetranuclear iron(III) complexes with amino acids involving a planar (μ-oxo)(μ-hydroxo)bis(μ-alkoxo)bis(μ-carboxylato)tetrairon core †

Tomoaki Tanase,*[a] Tomoko Inagaki,[a] Yasuko Yamada,[a] Masako Kato,[a] Emi Ota,[a] Mikio Yamazaki,[b] Mitsunobu Sato,[c] Wasuke Mori,[d] Kazuya Yamaguchi,[d] Masahiro Mikuriya,[e] Masashi Takahashi,[f] Masuo Takeda,[f] Isamu Kinoshita[g] and Shigenobu Yano*[a]

[a] *Department of Chemistry, Faculty of Science, Nara Women's University, Nara 630, Japan*
[b] *X-Ray Research Institute, Rigaku Corporation, Akishima, Tokyo 196, Japan*
[c] *Department of General Chemistry, Faculty of Engineering, Kogakuin University, Hachioji, Tokyo 192, Japan*
[d] *Department of Chemistry, Faculty of Science, Osaka University, Toyonaka, Osaka 560, Japan*
[e] *Department of Chemistry, School of Science, Kwansei Gakuin University, Nishinomiya-shi, Hyogo 514, Japan*
[f] *Department of Chemistry, Faculty of Science, Toho University, Miyama 2-2-1, Funabashi, Chiba 274, Japan*
[g] *Department of Chemistry, Faculty of Science, Osaka City University, Sumiyoshi-ku, Osaka 662, Japan*

Reactions of $Fe^{III}(NO_3)_3 \cdot 9H_2O$ with 0.5 equivalent of 2-hydroxypropane-1,3-diamine-*N*,*N*,*N*′,*N*′-tetraacetic acid (H_5dhpta) and an excess of amino acid [glycine (Gly) or L-alanine (L-Ala)] in water with the pH adjusted to *ca*. 5 by a solution of NaOH gave pale green crystals formulated as $Na[Fe_4(dhpta)_2(\mu\text{-}O)(\mu\text{-}OH)(O_2CCHRNH_3)_2]$ (R = H **1** or CH_3 **2**) in moderate yields. The tetrairon(III) complexes were characterized by elemental analyses, IR and ^{57}Fe Mössbauer spectra, variable-temperature magnetic susceptibility, and X-ray crystallographic and absorption analyses. The structure of **2**·$6H_2O$ was determined by X-ray crystallography to comprise a (μ-oxo)(μ-hydroxo)-bis(μ-alkoxo)bis(μ-carboxylato)tetrairon(III) cluster core bridged by two dhpta and two amino acid ligands. Two identical dinuclear iron(III) units [Fe(1)Fe(2) and Fe(3)Fe(4)] are each co-ordinated by a pentadentate dhpta ligand. The Fe(1) and Fe(4) are then bridged by the carboxylate of an amino acid and an oxo group, with the Fe(2) and Fe(3) similarly linked. The central two oxo groups are protonated to form a strongly hydrogen bonded $(O{-}H{-}O)^{3-}$ bridge [O · · · O 2.426(4) Å]. The average Fe · · · Fe distance for the μ-alkoxo dinuclear units is 3.692 Å (intradimer) and that for the bis(μ-carboxylato)(μ-oxo/hydroxo)diiron units is 3.463 Å (interdimer), both being in accord with the corresponding values from EXAFS analyses. The two L-alanine moieties are in zwitterionic form and act as interdimer bridging ligands with the carboxylate groups. The Na^+ counter cation is well packed between the tetrairon(III) complex anions, resulting in an infinite chain aggregation. The ^{57}Fe Mössbauer spectrum for **2**·$6H_2O$ clearly demonstrated that the four iron sites are equivalent, being in a high-spin octahedral iron(III) state. The variable-temperature magnetic susceptibility measurement for **2**·$6H_2O$ showed modest antiferromagnetism with an interdimer coupling constant (J) of -42.3 cm^{-1} and an intradimer coupling constant (J') of -20.8 cm^{-1}.

Extensive studies have recently focused on the (μ-oxo)(μ-carboxylato)diiron complexes as structural and functional synthetic models for the active sites of non-heme diiron proteins, hemerythrin (Hr), ribonucleotide reductase (RR), methane monooxygenase (MMO), and purple acid phosphatase (PAP).[1–3] The oxo- and carboxylate-bridged tri-, tetra- and higher nuclear iron clusters have also attracted attention as intermediate species of the iron storage protein, ferritin, many attempts leading to successful isolations of various structural and topological iron clusters.[1,4–7] In particular, those involving two oxo or hydroxo bridging groups with a short O · · · O distance have significant structural relationships with postulated intermediates of the oxygen-evolving centre (OEC) of photosystem II (PS II) which has been shown to contain a tetranuclear manganese cluster.[8–11] In this regard, we have been interested in the bis(μ-oxo)bis(μ-alkoxo)bis(μ-carbonato)tetrairon(III) complex, $Na_6[Fe_4(dhpta)(\mu\text{-}O)_2(\mu\text{-}CO_3)_2]$[12] [$H_5$dhpta = 2-hydroxypropane-1,3-diamine-*N*,*N*,*N*′,*N*′-tetraacetic acid (2-hydroxytrimethylenedinitrilotetraacetic acid)], since it involves a very short intramolecular non-bonded oxygen–oxygen contact of 2.408(9) Å between the central bis(μ-oxo) groups and is of potential importance in relation to the mechanism of the water oxidation process in PS II which involves a tetramanganese core. We have studied its dinuclear ruthenium(III)[13,14] and iron(III)[15] chemistry, and in this work amino acids were introduced as auxiliary interdimer bridging ligands to form a new series of tetranuclear complexes $Na[Fe_4(dhpta)_2(\mu\text{-}O)(\mu\text{-}OH)(\mu\text{-amino acid})_2]$, which were characterized by X-ray absorption and crystallographic analyses, Mössbauer spectroscopy, and variable-temperature magnetic measurement. The use of amino acids as bridging ligands in iron cluster chemistry is not common in spite of their potential bio-relevance.[16,17] Preliminary results have been reported.[18]

Experimental

Materials

All reagents were of the best commercial grade used as received. 2-Hydroxypropane-1,3-diamine-*N*,*N*,*N*′,*N*′-tetraacetic acid was from Aldrich.

† *Non-SI units employed*: eV ≈ 1.60×10^{-19} J, $\mu_B \approx 9.27 \times 10^{-24}$ J T^{-1}.

Measurements

Infrared spectra were measured on KBr pellets by using a JEOL FT/IR8300 spectrometer. The ratio of Fe : Na was determined by inductively coupled plasma (ICP) atomic emission spectroscopy on a SEIKO SPS 7700 plasma spectrometer by using $K_3[Fe(CN)_6]$ and NaCl as references and water as solvent. Magnetic susceptibility data were measured by the Faraday method over the range 4–300 K with a Cahn 1000 RH electrobalance. Susceptibilities at room temperature were also obtained by the Gouy method. The diamagnetic corrections were calculated from tables of Pascal's constants.[19] The temperature dependence of the molar susceptibility data was analysed by least-squares fit using the theoretical equation (1),[12]

$$\chi_m = (P/Q)Ng^2\beta^2/2k(T - \theta) + \text{t.i.p.} + \chi_{para} \qquad (1)$$

where $\theta = 2(J'/k)(P/Q)$, $P = 2e^A + 10e^B + 28e^C + 60e^D + 110e^E$, $Q = 1 + 3e^A + 5e^B + 7e^C + 9e^D + 11e^E$, $A = 2J/kT$, $B = 6J/kT$, $C = 12J/kT$, $D = 20J/kT$, $E = 30J/kT$, t.i.p. = temperature-independent paramagnetism, and $\chi_{para} = n_{par}S(S + 1)(Ng^2\beta^2/3kT)$; χ_{para} accounts for the spin-only magnetism associated with a paramagnetic impurity of mole percentage n_{par} and spin, and N = Avogadro's number, β = Bohr magneton, and k = Boltzmann's constant.

The ^{57}Fe Mössbauer spectra of a powdered sample for complex **2**·6H_2O at room temperature were obtained using a Mössbauer driving system from Wissenschaftliche Electronik and a ^{57}Co (Rh) Mössbauer source (1.5 GBq) from Amersham International plc. Details of the spectrometer have been described.[20] The spectra were fitted by Lorentzian lines on a personal computer and the isomer shifts are given relative to α-iron foil.

Preparation of Na[Fe_4(dhpta)$_2$(μ-O)(μ-OH)(μ-amino acid)$_2$] (amino acid = Gly 1 or L-Ala 2)

Compounds $Fe(NO_3)_3$·9H_2O (1.0 mmol) and H_5dhpta (0.5 mmol) were dissolved in water (40 cm^3) at 70 °C and the pH of the solution was adjusted to *ca.* 5 with 1 M NaOH solution. Amino acid (Gly or L-Ala) was then added and the pH again adjusted to *ca.* 5. Slow evaporation, taking several days, afforded pale green crystals of Na[Fe_4(dhpta)$_2$(μ-O)(μ-OH)(μ-amino acid)$_2$]·solv, which were collected, washed with a small amount of cold water, acetone and diethyl ether, and dried *in vacuo*. Complex **1**·8H_2O (amino acid = glycine): yield 46% (Found: C, 25.65; H, 4.05; N, 6.95. Calc. for $C_{26}H_{51}Fe_4N_6NaO_{32}$: C, 25.85; H, 4.42; N, 6.96%; IR (KBr) $\tilde{\nu}$/cm^{-1} 1639, 1489, 1378, 1339 and 744. Complex **2**·6H_2O (amino acid = L-alanine): yield 54% (Found: C, 27.97; H, 4.87; N, 7.09. Calc. for $C_{28}H_{53}Fe_4N_6NaO_{30}$: C, 28.02; H, 4.45; N, 7.00%); IR (KBr) $\tilde{\nu}$/cm^{-1} 1641, 1464, 1368, 1322 and 739.

X-Ray absorption analyses

X-Ray absorption measurements around the iron K edge (6.4–8.4 keV with 700 steps) were performed at the Photon Factory of the National Laboratory for High Energy Physics on beam line 10B using synchrotron radiation (2.5 GeV, 340–300 mA).[21] The experiments were done in the transmission mode on powdered samples as BN pellets using a Si(311) monochromator. The theoretical expression of the obtained $k^3\chi(k)$ for the case of single scattering is shown in equation (2),[22] where r_i, N_i, S_i, $F_i(k)$,

$$k^3\chi(k) = \sum_i \left\{ \frac{k^2 N_i}{r_i^2} S_i F_i(k) \exp(-2\sigma_i^2 k^2) \sin[2kr_i + \varphi_i(k)] \right\} \qquad (2)$$

$\varphi_i(k)$ and σ_i represent the interatomic distance, co-ordination number, reduction factor, back-scattering amplitude, phase shift and Debye–Waller factor, respectively, and k is the photoelectron wavevector defined as $[(2m/\hbar^2)(E - E_0)]^{\frac{1}{2}}$ (E_0 = 7126 eV). The back-scattering amplitude $F_i(k)$ and the phase shift $\varphi_i(k)$ functions used were the theoretical parameters tabulated by McKale *et al.*[23] Parameters, N_i, r_i, E_0 and σ_i were varied in the non-linear least-squares refined curve fitting, and fixed values of S_i were used which were determined from an analysis of the structurally characterized compound $Na_3[Fe_4(dhpta)_2(\mu\text{-}O)(\mu\text{-}OH)\{O_2CC(CH_3)=CH_2\}_2]$·8$H_2O$,‡ by using fixed N_i values, $N_{N/O} = 6$, $N_C = 7$, and $N_{Fe} = N_{Fe'} = 1$. Fourier-filtered (r = 0.8–3.9 Å) EXAFS data, $k^3\chi(k)_{obs}$, were analysed with four waves, $k^3\chi(k)_{calc} = k^3\chi_{N/O} + k^3\chi_C + k^3\chi_{Fe} + k^3\chi_{Fe'}$ in a k space of 2.5–14.0 $Å^{-1}$. The first co-ordinated atoms, 5O + 1N, were treated as oxygen. All calculations were performed on an IBM P-120 computer with the EXAFS analysis program package, REX (Rigaku).[24]

X-Ray crystallography

The crystal of complex **2**·6H_2O used was mounted on the end of a glass fibre and the data collection was carried out at 20 °C on a Rigaku AFC7R diffractometer equipped with graphite-monochromated Mo-Kα (λ = 0.710 69 Å) radiation. Crystal data and experimental conditions are listed in Table 1. Three standard reflections were monitored every 150 and showed no systematic decrease in intensity. Reflection data were corrected for Lorentz-polarization effects and an absorption correction was applied by the ψ-scan method. The known absolute configuration of L-alanine was used as an internal reference asymmetric centre to determine the absolute configuration of the crystal.

The structure was solved by direct methods with SAPI 91.[25] Most non-hydrogen atoms were located initially and subsequent Fourier-difference syntheses gave the remainder. The C–H hydrogen atoms were placed at ideal positions with a distance of 0.95 Å and the N–H and O–H hydrogen atoms except those of water molecules were determined by Fourier-difference syntheses. All hydrogen atoms were fixed in the refinement. The structure was refined on F_o with full-matrix least-square techniques minimizing $\Sigma w(|F_o| - |F_c|)^2$. Final refinement with anisotropic thermal parameters for all non-hydrogen atoms converged at $R = 0.035$ and $R' = 0.050$, where $R = \Sigma||F_o| - |F_c||/\Sigma|F_o|$ and $R' = [\Sigma w(|F_o| - |F_c|)^2/\Sigma w|F_o|^2]^{\frac{1}{2}}$ and $w = 1/\sigma^2(F_o)$. The

Table 1 Crystallographic and experimental data for Na[Fe_4(dhpta)$_2$(μ-O)(μ-OH)(μ-L-Ala)$_2$]·6H_2O (**2**·6H_2O)

Formula	$C_{28}H_{53}Fe_4N_6NaO_{30}$
M	1200.13
Crystal system	Monoclinic
Space group	$P2_1$ (no. 4)
a/Å	11.762(1)
b/Å	15.924(2)
c/Å	12.948(2)
β/°	109.46(1)
U/$Å^3$	2286.6(5)
Z	2
T/°C	20
D_c/g cm^{-3}	1.743
μ/cm^{-1}	13.56
2θ Range/°	4–60
Scan method	ω–2θ
Scan speed/° min^{-1}	16
No. unique data	6890
No. observed data [$I > 3\sigma(I)$]	5255
No. variables	622
R	0.035
R'	0.050
Goodness of fit *	1.10

* $[\Sigma w(|F_o| - |F_c|)^2/(N_o - N_p)]^{\frac{1}{2}}$ where N_o = number of data, N_p = number of variables.

‡ The structure, analogous to that of **2**, was determined by X-ray crystallography: monoclinic, space group $C2/m$, $a = 27.067(3)$, $b = 20.480(5)$, $c = 11.797(3)$ Å, $U = 6225(2)$ $Å^3$, $Z = 4$, $R = 0.063$, $R' = 0.088$; Fe–Fe 3.448(9), 3.703(2) Å, average Fe–O/N 2.02, Fe–C 2.94 Å. Details will be reported in a subsequent paper.

Table 2 Structural parameters derived from EXAFS analyses

		EXAFS				Crystallography	
Complex	Shell	N^a	r^b/Å	σ	R^c	r (average)/Å	N
$Na[Fe_4(dhpta)_2(\mu\text{-}O)(\mu\text{-}OH)(\mu\text{-}Ala)_2]\cdot 6H_2O$ (**2**·$6H_2O$)	Fe–O/N[d]	6.3	2.07	0.095	0.057	2.03	6
	Fe–C	6.9	2.94	0.074		2.94	7
	Fe···Fe	0.5	3.42	0.043		3.463	1
	Fe···Fe′	0.5	3.71	0.086		3.692	1
$Na[Fe_4(dhpta)_2(\mu\text{-}O)(\mu\text{-}OH)(\mu\text{-}Gly)_2]\cdot 8H_2O$ (**1**·$8H_2O$)	Fe–O/N[d]	6.9	2.06	0.097	0.062		
	Fe–C	8.4	2.94	0.088			
	Fe···Fe	0.4	3.41	0.016			
	Fe···Fe′	0.7	3.68	0.100			

[a] Complex $Na_3[Fe_4(dhpta)_2(\mu\text{-}O)(\mu\text{-}OH)\{\mu\text{-}O_2CC(CH_3)=CH_2\}_2]\cdot 8H_2O$ was used as reference to determine the reduction factors S_i. [b] Estimated errors are ±0.03 Å for the first shell and ±0.04 Å for outer shells. [c] $R = \{\Sigma[k^3\chi(k)_{obs} - k^3\chi(k)_{calc}]^2/\Sigma[k^3\chi(k)_{obs}]^2\}^{\frac{1}{2}}$. [d] All back-scattering atoms in the first shell are calculated as oxygen.

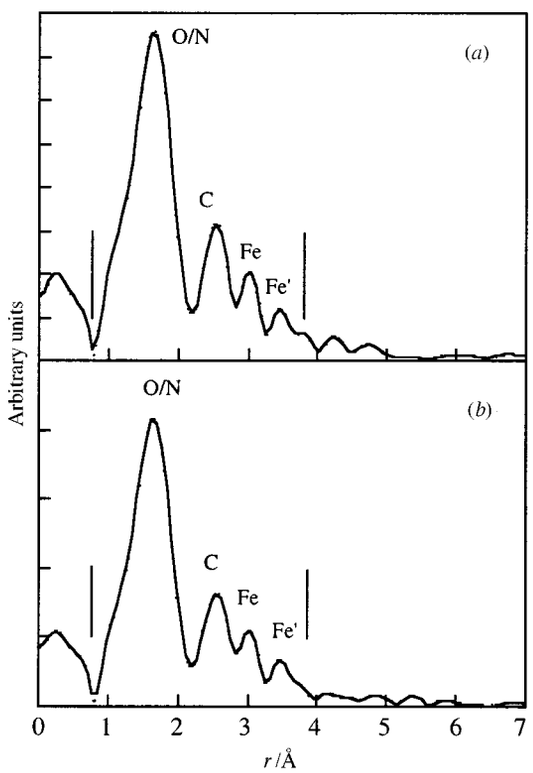

Fig. 1 Fourier transforms over $k = 2.5$–14 Å^{-1} of the k^3-weighted EXAFS data (before phase-shift correction) for complexes (*a*) **2**·$6H_2O$ and (*b*) **1**·$8H_2O$

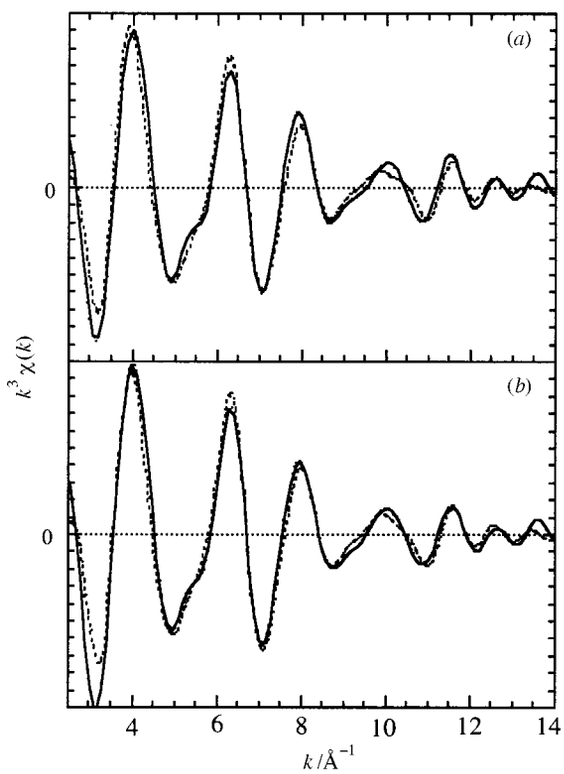

Fig. 2 Curve fits over the range $k = 2.5$–14 Å^{-1} to the Fourier-filtered data ($r = 0.8$–3.9 Å) for complexes (*a*) **2**·$6H_2O$ and (*b*) **1**·$8H_2O$. ——, Fourier-filtered EXAFS data; – – –, calculated data

final Fourier-difference map showed maximum and minimum peaks of 0.32 and −0.20 e Å^{-3}, respectively.

Atomic scattering factors and values of f' and f'' for Fe, Na, O, N and C were taken from refs. 26 and 27. All calculations were carried out on a Silicon Graphics Indigo computer with the TEXSAN program package.[28]

CCDC reference number 186/814.

Results and Discussion

Preparation of $Na[Fe_4(dhpta)_2(\mu\text{-}O)(\mu\text{-}OH)(\mu\text{-amino acid})_2]$

Reactions of $Fe^{III}(NO_3)_3\cdot 9H_2O$ with 0.5 equivalent of 2-hydroxypropane-1,3-diamine-*N*,*N*,*N*′,*N*′-tetraacetic acid and excess of amino acid (glycine or L-alanine) in water with the pH adjusted to *ca.* 5 by NaOH afforded pale green crystals formulated as $Na[Fe_4(dhpta)_2(\mu\text{-}O)(\mu\text{-}OH)(O_2CCHRNH_3)_2]$ (R = H **1** or CH_3 **2**) in moderate yields (46–54%). Complexes **1** and **2** were not soluble in most organic solvents except dimethylformamide, and sparingly soluble in water. The elemental analyses indicated the presence of one dhpta and one amino acid ligand per two iron atoms. The ratio of Na : Fe for complex **2** was determined by ICP spectroscopy as 1 : 4, suggesting a tetranuclear iron structure. The IR spectra of **1** and **2** were similar and indicated the presence of carboxylate and dhpta ligands with bands at around 1641–1322 cm^{-1}

EXAFS analyses

The X-ray absorption spectra around the iron K edge were measured for powdered samples of **1** and **2**, and EXAFS (extended X-ray absorption fine structure) analyses were carried out to determine the metal framework. The Fourier transforms of the EXAFS data for **1** and **2** are shown in Fig. 1. The spectra are closely similar, and four distinct peaks were observed at about 1.6, 2.5, 3.0 and 3.5 Å (before phase-shift correction), which were assigned to the back-scattering contributions of the nitrogen and oxygen atoms (N/O) co-ordinating to iron, the carbon atoms (C) including five-membered chelate rings, and the outer two iron atoms (Fe), respectively, by Fourier-filtered pre-curve-fitting analyses. The N and O atoms involved in the first co-ordination sphere could not be distinguished in the present analyses. The Fourier-filtered (r =

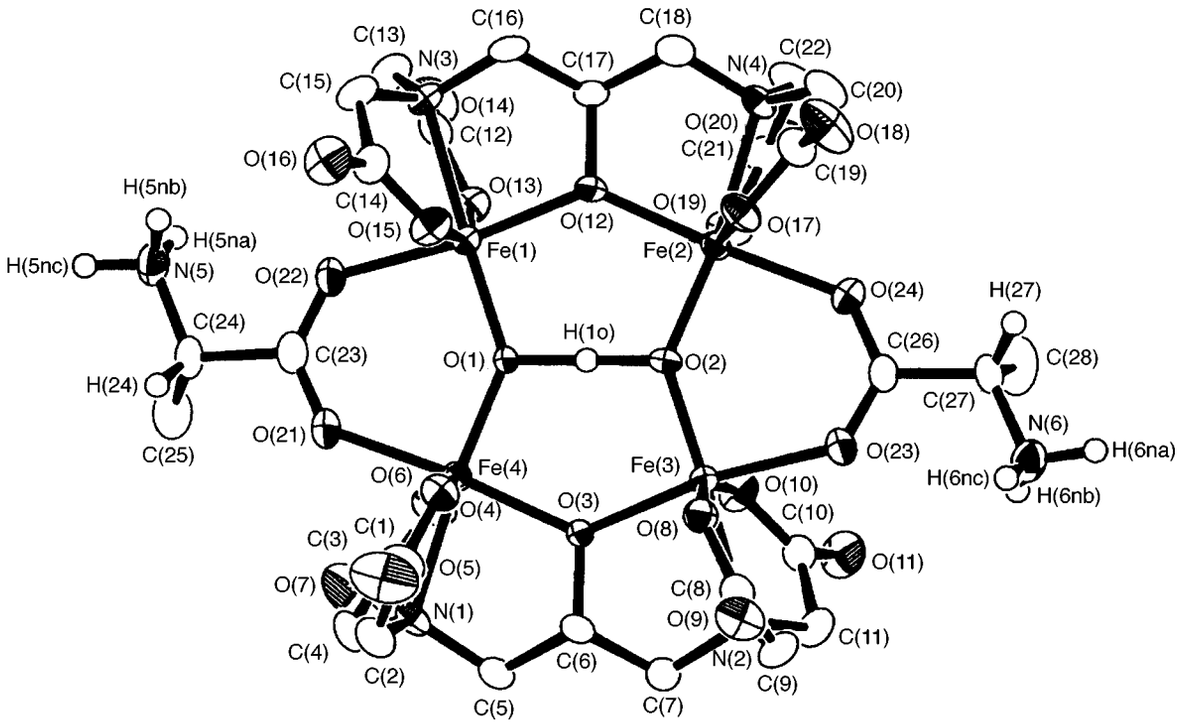

Fig. 3 An ORTEP plot of the complex anion of $Na[Fe_4(dhpta)_2(\mu\text{-}O)(\mu\text{-}OH)(\mu\text{-}Ala)_2]\cdot 6H_2O$ ($\mathbf{2}\cdot 6H_2O$)

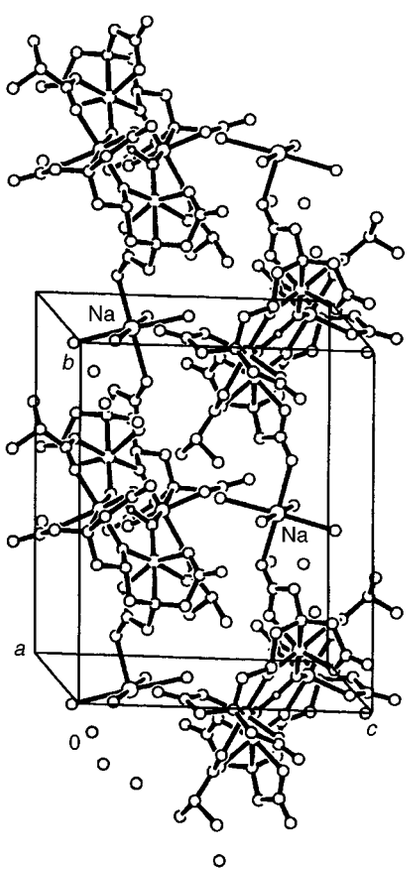

Fig. 4 Crystal packing of compound $\mathbf{2}\cdot 6H_2O$

0.8–3.9 Å) EXAFS data, $k^3\chi(k)_{obs}$, were subjected to curve-fitting analyses with a four-wave model, $k^3\chi(k)_{calc} = k^3\chi(k)_{N/O} + k^3\chi(k)_C + k^3\chi(k)_{Fe} + k^3\chi(k)_{Fe'}$ (Fig. 2). The structural parameters derived from EXAFS analyses are summarized in Table 2. The iron ions were assumed to have octahedral geometry on the basis of N (6.3–6.9) for the first shell. A tetranuclear cluster core might be inferred from the two iron backscattering peaks at 3.41–3.42 and 3.68–3.71 Å, the former corresponding to Fe···Fe distances involved in oxo- or hydroxo-bridged dinuclear iron(III) complexes and the latter to those of dhpta-bridged (μ-alkoxo)diiron(III) complexes.

Crystal structure of $Na[Fe_4(dhpta)_2(\mu\text{-}O)(\mu\text{-}OH)(\mu\text{-}L\text{-}Ala)_2]\cdot 6H_2O$ ($2\cdot 6H_2O$)

The structure of complex $\mathbf{2}\cdot 6H_2O$ was determined by X-ray crystallography. An ORTEP[29] diagram of the complex cation with the atomic numbering scheme is given in Fig. 3 and selected bond lengths and angles are listed in Table 3. The asymmetric unit contains a complex anion, a sodium cation and six water molecules. The complex anion consists of four iron atoms bridged by two dhpta and two amino acid ligands and an oxo–hydroxo unit. In other words, two dhpta-bridged diiron(III) dimers are combined by two carboxylate bridges of L-alanine moieties and two oxo-bridges in which a proton is symmetrically included, leading to a planar (μ-oxo)(μ-hydroxo)bis(μ-alkoxo)bis(μ-carboxylato)tetrairon(III) cluster core. The four iron atoms deviate from their best least-squares plane only by 0.003–0.007 Å, and the bridging oxygen atoms [O(1), O(2), O(3) and O(12)] are nearly coplanar with deviations of 0.120–0.178 Å. The average Fe···Fe distance for the μ-alkoxo dinuclear units is 3.692 Å and that for the bis(μ-carboxylato)(μ-oxo/hydroxo)diiron units is 3.463 Å, both being in accord with the corresponding values from EXAFS analyses. The four iron(III) ions are equivalent, consistent with the Mössbauer spectrum (see below), and are octahedrally coordinated by a O_5N donor set. The μ-oxo-diiron(III) character in the Fe(4)–O(1)–Fe(1) and Fe(2)–O(2)–Fe(3) units is appreciably reduced owing to a symmetrical protonation, H(1o), between the O(1) and O(2) atoms. The Fe–O(1 or 2) bond lengths are 1.850(4)–1.862(4) Å (average 1.854 Å), which are significantly longer than those of typical μ-oxo–diiron(III) complexes (1.76–1.82 Å)[2,30,31] and slightly longer than those of $Na_6[Fe_4(dhpta)_2O_2(CO_3)_2]$ **3** (average 1.829 Å).[12] The average Fe–O(1 or 2)–Fe angle of 138.1° is comparable to that in **3** [136.4(3)°]. The *trans* effect of the bridging oxo group is also reduced by the protonation, resulting in a slight elongation of the Fe–N bonds (average 2.190 Å) compared with the corresponding values (average 2.184 Å) found in the dhpta-bridged diiron(III) complexes $[Fe_2(dhpta)(O_2CR)(H_2O)_2]$ (R = C_6H_5 **4a**, C_6H_4OH **4b** or

Table 3 Selected bond distances (Å) and angles (°) for $Na[Fe_4(dhpta)_2(\mu\text{-}O)(\mu\text{-}OH)(\mu\text{-}L\text{-}Ala)_2]\cdot 6H_2O$ (**2**·$6H_2O$) with estimated standard deviations in parentheses

Fe(4)···Fe(1)	3.474(1)	Fe(4)···Fe(3)	3.675(1)	Fe(2)–O(24)	2.079(6)	Fe(2)–N(4)	2.203(4)
Fe(1)···Fe(2)	3.709(1)	Fe(2)···Fe(3)	3.451(1)	Fe(3)–O(2)	1.850(4)	Fe(3)–O(3)	2.016(4)
Fe(4)–O(1)	1.862(4)	Fe(4)–O(3)	2.011(4)	Fe(3)–O(8)	2.012(4)	Fe(3)–O(10)	2.010(5)
Fe(4)–O(4)	2.011(4)	Fe(4)–O(6)	2.023(5)	Fe(3)–O(23)	2.082(5)	Fe(3)–N(2)	2.195(5)
Fe(4)–O(21)	2.062(6)	Fe(4)–N(1)	2.190(4)	Na(1)–O(11)	2.414(7)	Na(1)–O(16*)	2.417(7)
Fe(1)–O(1)	1.853(4)	Fe(1)–O(12)	2.017(4)	Na(1)–O(31)	2.573(7)	Na(1)–O(32)	2.623(7)
Fe(1)–O(13)	2.020(4)	Fe(1)–O(15)	2.036(5)	Na(1)–O(33)	2.409(6)	Na(1)–O(34)	2.382(6)
Fe(1)–O(22)	2.101(4)	Fe(1)–N(3)	2.172(5)	O(1)···O(2)	2.426(4)	O(1)–H(1o)	1.22
Fe(2)–O(2)	1.850(4)	Fe(2)–O(12)	2.033(5)	O(2)–H(1o)	1.21		
Fe(2)–O(17)	2.028(5)	Fe(2)–O(19)	2.015(5)				
Fe(1)···Fe(4)···Fe(3)	89.09(2)	Fe(4)···Fe(1)···Fe(2)	90.55(3)	O(2)–Fe(2)–O(19)	103.8(2)	O(2)–Fe(2)–O(24)	92.5(2)
Fe(1)···Fe(2)···Fe(3)	88.88(3)	Fe(4)···Fe(3)···Fe(2)	91.48(3)	O(2)–Fe(2)–N(4)	173.1(2)	O(12)–Fe(2)–O(17)	95.5(2)
O(1)–Fe(4)–O(3)	92.5(2)	O(1)–Fe(4)–O(4)	102.5(2)	O(12)–Fe(2)–O(19)	90.3(2)	O(12)–Fe(2)–O(24)	175.4(2)
O(1)–Fe(4)–O(6)	102.5(2)	O(1)–Fe(4)–O(21)	92.6(2)	O(12)–Fe(2)–N(4)	82.1(2)	O(17)–Fe(2)–O(19)	153.1(2)
O(1)–Fe(4)–N(1)	174.5(2)	O(3)–Fe(4)–O(4)	91.3(2)	O(17)–Fe(2)–O(24)	86.1(2)	O(17)–Fe(2)–N(4)	76.5(2)
O(3)–Fe(4)–O(6)	95.8(2)	O(3)–Fe(4)–O(21)	174.9(2)	O(19)–Fe(2)–O(24)	86.4(2)	O(19)–Fe(2)–N(4)	78.3(2)
O(3)–Fe(4)–N(1)	82.2(2)	O(4)–Fe(4)–O(6)	153.7(2)	O(24)–Fe(2)–N(4)	94.2(2)	O(2)–Fe(3)–O(3)	95.2(2)
O(4)–Fe(4)–O(21)	87.2(2)	O(4)–Fe(4)–N(1)	79.0(2)	O(2)–Fe(3)–O(8)	101.8(2)	O(2)–Fe(3)–O(10)	101.5(2)
O(6)–Fe(4)–O(21)	83.4(2)	O(6)–Fe(4)–N(1)	77.0(2)	O(2)–Fe(3)–O(23)	94.4(2)	O(2)–Fe(3)–N(2)	177.9(2)
O(21)–Fe(4)–N(1)	92.7(2)	O(1)–Fe(1)–O(12)	93.9(2)	O(3)–Fe(3)–O(8)	90.8(2)	O(3)–Fe(3)–O(10)	93.2(2)
O(1)–Fe(1)–O(13)	102.1(2)	O(1)–Fe(1)–O(15)	101.7(2)	O(3)–Fe(3)–O(23)	170.3(2)	O(3)–Fe(3)–N(2)	82.8(2)
O(1)–Fe(1)–O(22)	93.5(2)	O(1)–Fe(1)–N(3)	177.3(2)	O(8)–Fe(3)–O(10)	155.8(2)	O(8)–Fe(3)–O(23)	86.4(2)
O(12)–Fe(1)–O(13)	91.0(2)	O(12)–Fe(1)–O(15)	93.3(2)	O(8)–Fe(3)–N(2)	78.9(2)	O(10)–Fe(3)–O(23)	85.6(2)
O(12)–Fe(1)–O(22)	172.5(2)	O(12)–Fe(1)–N(3)	83.4(2)	O(10)–Fe(3)–N(2)	78.0(2)	O(23)–Fe(3)–N(2)	87.6(2)
O(13)–Fe(1)–O(15)	155.4(2)	O(13)–Fe(1)–O(22)	86.1(2)	Fe(4)–O(1)–Fe(1)	138.4(3)	Fe(2)–O(2)–Fe(3)	137.8(3)
O(13)–Fe(1)–N(3)	78.3(2)	O(15)–Fe(1)–O(22)	86.5(2)	Fe(4)–O(3)–Fe(3)	131.7(2)	Fe(1)–O(12)–Fe(2)	132.6(2)
O(15)–Fe(1)–N(3)	78.2(2)	O(22)–Fe(1)–N(3)	89.2(2)	O(1)–H(1o)–O(2)	176.0		
O(2)–Fe(2)–O(12)	91.3(2)	O(2)–Fe(2)–O(17)	102.3(2)				

$CH_2CH{=}CH_2$ **4c**).[15] The H(1o) atom was unambiguously determined by a Fourier-difference synthesis at an almost central position of the tetranuclear core, O(1)–H(1o) 1.22, O(2)–H(1o) 1.21 Å and O(1)–H(1o)–O(2) 176.0°. The interatomic distance between the O(1) and O(2) atoms is 2.426(4) Å, indicating a strong hydrogen bond. A similar short contact has been observed in the (μ-O)(μ-OH) system of the tetramanganese complex $[Mn_4(dhpta)_2(\mu\text{-}O)(\mu\text{-}OH)(\mu\text{-}O_2CCH_3)_2]^{4-}$ **5**,[32] and the (μ-OH)(μ-OH) system of the hexanuclear iron(III) complex $[Fe_6(\mu_3\text{-}O)_2(\mu\text{-}OH)_2(H_2O)_2(\mu\text{-}O_2CPh)_{12}(diox)]$ **6** (diox = 1,4-dioxane)[33] as well as in **3**. The structural similarity between **2** and **3** strongly suggested that complex **3** reported as $Na_6[Fe_4(dhpta)_2(\mu\text{-}O)_2(\mu\text{-}CO_3)_2]$ involved a $\mu\text{-}(O{-}H{-}O)^{3-}$ protonated centre as the authors noted. The complex **2** is, therefore, the first structurally characterized example of the tetrairon(III) complex having a bridging $(O{-}H{-}O)^{3-}$ unit, which could be of special interest in relevance to the mechanism of water oxidation by the Mn_4 cluster in the OEC of photosystem II and its synthetic and theoretical approaches.[34]

The dhpta-bridged dimer structures are essentially similar to those of complexes **4**. The average $Fe{-}O_{alkoxo}$ bond length is 2.020 Å, slightly longer than those of **4** [1.971(4)–2.006(2) Å], and the $Fe{-}O_{alkoxo}{-}Fe$ angle is 132.2°, slightly larger than those of **4** [129.30(7)–130.2(2)°].[15] The small difference should be caused by the presence of the intradimer carboxylate bridge in **4**. The two L-alanine moieties are in zwitterionic form, protonated amino groups being demonstrated by the Fourier-difference syntheses, and act as interdimer bridging ligands with the carboxylate groups. The $Fe{-}O_{ala}$ bond lengths, 2.062(6)–2.101(4) Å (average 2.081 Å), are longer than those for the anionic ligands, CO_3^{2-} and RCO_2^-, found in **3** and **4**.[12,15]

The Na^+ counter cation is well packed between the tetrairon(III) complex anions in the lattice, resulting in an infinite chain aggregation, Na–[Fe_4]–Na··· (Fig. 4). The Na(1) atom is co-ordinated by four water molecules and two acetate oxygen atoms [O(11) and O(16*)] belonging to different complex anions.

Mössbauer spectrum

The ^{57}Fe Mössbauer spectrum for complex **2**·$6H_2O$ is illustrated in Fig. 5 together with the fitted curve. The spectrum consists of an almost symmetric quadrupole doublet with small linewidths (Γ = 0.38–0.40 mm s^{-1}), clearly demonstrating that the four iron sites are equivalent. The isomer shift (δ), 0.36 mm s^{-1}, and quadrupole splitting (Δ), 1.21 mm s^{-1}, are within the range expected for high-spin octahedral iron(III) ions.[35] The values of Δ are notably smaller than those observed in μ-oxo dinuclear iron(III) complexes (1.50–1.72 mm s^{-1} at liquid-nitrogen temperature),[36–38] which would be ascribed to the less distorted octahedral co-ordination for **2**·$6H_2O$, resulting from the protonation of the bis(μ-oxo) unit, in comparison with those for the μ-oxo dinuclear complexes having significantly short $Fe{-}O_{oxo}$ bonds. Indeed the μ-hydroxo dinuclear iron(III) complex $[Fe_2(OH)(O_2CCH_3)_2\{HB(pz)_3\}_2]ClO_4$ exhibited a very small Δ value of 0.25 mm s^{-1} at 80 K,[37] while the μ-oxo dinuclear complex $[Fe_2O(O_2CCH_3)_2\{HB(pz)_3\}_2]$ one of 1.60 mm s^{-1} at 4.2 K.[38]

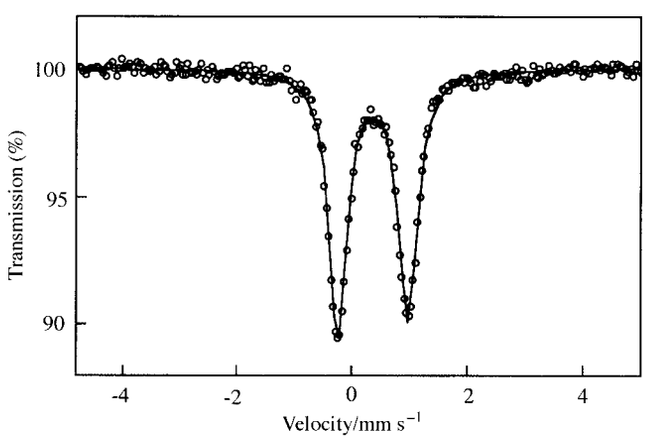

Fig. 5 The ^{57}Fe Mössbauer spectrum of complex **2**·$6H_2O$ at room temperature. Circles represent experimental data and the solid line is the best fit

Magnetic properties

The temperature-dependent magnetic susceptibility per Fe^{III}

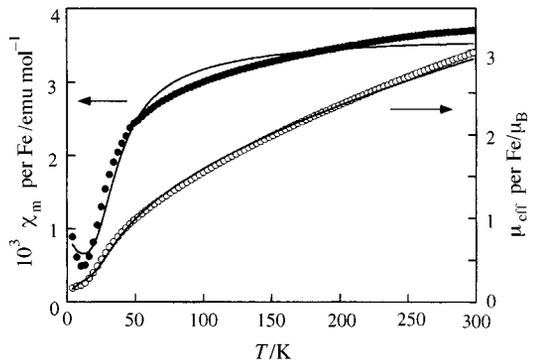

Fig. 6 Temperature dependence of the magnetic susceptibility per Fe^{III} and magnetic moment per Fe^{III} for complex **2**·$6H_2O$. Circles represent experimental data and solid lines the best fits

and magnetic moment per Fe^{III} for complex **2**·$6H_2O$ in the range 4–300 K are shown in Fig. 6. The molar susceptibility data were fitted by the theoretical equation (1) in the Experimental section to produce $J = -42.3$ cm^{-1}, $J' = -20.8$ cm^{-1}, and t.i.p. = 595×10^{-6} emu mol^{-1} (7.48×10^{-9} cm^3 mol^{-1}) with g fixed at 2.0. The increase in χ_m below 20 K could result from the presence of a high-spin iron(III) impurity which can be accounted by the χ_{para} term with $n = 0.02\%$ and $S = \frac{5}{2}$. The interdimer coupling J, occurring mainly through the partially protonated μ-oxo group, indicated a modest antiferromagnetic interaction but is significantly smaller than the values usually observed for oxo-bridged iron(III) dimers (−70 to −132 cm^{-1}),[2,30,31] tentatively due to the protonation between the two μ-oxo groups. The intradimer coupling J', occurring through the μ-alkoxo group, is typical of the weak antiferromagnetic interactions observed for iron(III) dinuclear complexes with hydroxo or alkoxo bridging (−7 to −26 cm^{-1}).[2,39–49] Complex **3**, reported as $Na_6[Fe_4(dhpta)_2(\mu\text{-}O)_2(\mu\text{-}CO_3)_2]$, also showed similar weak antiferromagnetic couplings with $J = -63.4$ cm^{-1} and $J' = -11.2$ cm^{-1}; the former interaction is slightly stronger and the latter weaker than those in the present complex.[12]

Conclusion

The dimer of dimers type tetranuclear iron(III) complexes $Na[Fe_4(dhpta)_2(\mu\text{-}O)(\mu\text{-}OH)(\mu\text{-}O_2CR)_2]$ were prepared by using amino acid ligands, and involve a (μ-O–H–O)bis(μ-alkoxo)bis(μ-carboxylato)tetrairon core. The novel, strongly hydrogen-bonded $(O–H–O)^{3-}$ bridging system was unambiguously characterized by an X-ray crystallographic analysis of **2**·$6H_2O$, and could provide very useful structural information in relation to the oxidation of water by OEC PS-II. The use of amino acids can also be advantageous, by introducing chirality and functional groups into the tetrairon core, in the development of functional clusters.

Acknowledgements

This work was partially supported by a Grant-in-Aid for Scientific Research from the Ministry of Education of Japan and Grants from the Iwatani, Nippon Itagarasu, Mitsubishi-Yuka and Nagase Foundations and the San-Ei Gen Foundation for Food Chemical Research.

References

1 S. J. Lippard, *Angew. Chem., Int. Ed. Engl.*, 1988, **27**, 344.
2 J. D. M. Kurtz, *Chem. Rev.*, 1990, **90**, 585.
3 A. L. Feig and S. J. Lippard, *Chem. Rev.*, 1994, **94**, 759.
4 K. Wieghardt, *Angew. Chem., Int. Ed. Engl.*, 1989, **28**, 1153.
5 K. S. Hagen, *Angew. Chem., Int. Ed. Engl.*, 1992, **31**, 1010.
6 K. L. Taft, C. D. Delfs, G. C. Papaefthymiou, S. Foner, D. Gatteschi and S. J. Lippard, *J. Am. Chem. Soc.*, 1994, **116**, 823.
7 K. L. Taft, G. C. Papaefthymiou and S. J. Lippard, *Inorg. Chem.*, 1994, **33**, 1510.
8 K. Wieghardt, *Angew. Chem., Int. Ed. Engl.*, 1994, **33**, 725.
9 V. L. Pecoraro, M. J. Baldwin and A. Gelasco, *Chem. Rev.*, 1994, **94**, 807.
10 V. K. Yachandra, V. J. DeRose, M. J. Latimer, I. Mukerji, K. Sauer and M. Klein, *Science*, 1993, **260**, 675.
11 V. J. DeRose, I. Mukerji, M. J. Latimer, V. K. Yachandra, K. Sauer and M. P. Klein, *J. Am. Chem. Soc.*, 1994, **116**, 5239.
12 D. L. Jameson, C.-L. Xie, D. N. Hendrickson, J. A. Potenza and H. J. Schugar, *J. Am. Chem. Soc.*, 1987, **109**, 740.
13 T. Tanase, M. Kato, Y. Yamada, K. Tanaka, K. Lee, Y. Sugihara, A. Ichimura, I. Kinoshita, M. Haga, Y. Sasaki, Y. Yamamoto, T. Nagano and S. Yano, *Chem. Lett.*, 1994, 1853.
14 T. Tanase, Y. Yamada, K. Tanaka, T. Miyazu, M. Kato, K. Lee, Y. Sugihara, W. Mori, A. Ichimura, I. Kinoshita, Y. Yamamoto, M. Haga, Y. Sasaki and S. Yano, *Inorg. Chem.*, 1996, **35**, 6230.
15 M. Kato, Y. Yamada, T. Inagaki, W. Mori, K. Sasai, T. Tsubomura, M. Sato and S. Yano, *Inorg. Chem.*, 1995, **34**, 2645.
16 T. Tokii, K. Ide, M. Nakashima and M. Koikawa, *Chem. Lett.*, 1994, 441.
17 Y. Sasaki, K. Umakoshi, S. Kimura, C.-E. Oh, M. Yamasaki and T. Shibahara, *Chem. Lett.*, 1994, 1185.
18 S. Yano, T. Inagaki, Y. Yamada, M. Kato, M. Yamasaki, K. Sakai, T. Tsubomura, M. Sato, W. Mori, K. Yamaguchi and I. Kinoshita, *Chem. Lett.*, 1996, 61.
19 B. N. Figgs and J. Lewis, *Modern Coordination Chemistry*, eds. J. Lewis and R. G. Wilkins, Interscience, New York, 1960, p. 403.
20 M. Takahashi, M. Takeda, K. Awaga, T. Okuno, Y. Maruyama, A. Kobayashi, H. Kobayashi, S. Schenk, N. Robertson and A. Underhill, *Mol. Cryst. Liq. Cryst.*, 1996, **286**, 77.
21 Photon Factory Activity Report, No. 3, National Laboratory for High Energy Physics, Ibaraki, 1986.
22 D. E. Sayers, E. A. Stern and F. W. Lytle, *Phys. Rev. Lett.*, 1971, **27**, 1204.
23 A. G. McKale, B. W. Veal, A. P. Paulikas, S. K. Chan and G. S. Knapp, *J. Am. Chem. Soc.*, 1988, **110**, 3763.
24 REX, Rigaku Corporation, Tokyo, 1995.
25 H.-F. Fan, R-SAPI 91, Structure Analysis Programs with Intelligent Control, Rigaku Corporation, Tokyo, 1988.
26 D. T. Cromer, *Acta Crystallogr.*, 1965, **18**, 17.
27 D. T. Cromer and J. T. Waber, *International Tables for X-Ray Crystallography*, Kynoch Press, Birmingham, 1974, vol. IV.
28 TEXSAN, Structure Analysis Package, Molecular Structure Corporation, The Woodlands, TX, 1985.
29 C. K. Johnson, ORTEP, Report ORNL-5138, Oak Ridge National Laboratory, Oak Ridge, TN, 1976.
30 J. A. Thich, B. H. Toby, D. A. Powers, J. A. Potenza and H. J. Schugar, *Inorg. Chem.*, 1981, **20**, 3314.
31 S. M. Gorun and S. J. Lippard, *Inorg. Chem.*, 1991, **30**, 1625.
32 R. T. Stibrany and S. M. Gorun, *Angew. Chem., Int. Ed. Engl.*, 1990, **29**, 1156.
33 W. Micklitz and S. J. Lippard, *Inorg. Chem.*, 1988, **27**, 3069.
34 D. M. Proserpio, R. Hoffman and C. Dismukes, *J. Am. Chem. Soc.*, 1992, **114**, 4374.
35 D. P. E. Dickson and F. J. Berry, *Mössbauer Spectroscopy*, Cambridge University Press, Cambridge, 1986.
36 K. S. Murray, *Coord. Chem. Rev.*, 1974, **12**, 1.
37 J. R. Hartman, R. L. Rardin, P. Chaudhuri, K. Pohl, K. Wieghardt, B. Nuber, J. Weiss, G. C. Papaefthymiou, R. B. Frankel and S. J. Lippard, *J. Am. Chem. Soc.*, 1987, **109**, 7387.
38 W. H. Armstrong, A. Spool, G. C. Papaefthymiou, R. B. Frankel and S. J. Lippard, *J. Am. Chem. Soc.*, 1984, **106**, 3653.
39 B. P. Murch, P. D. Boyle and J. L. Que, *J. Am. Chem. Soc.*, 1985, **107**, 6728.
40 B. A. Brennan, Q. Chen, C. Juarez-Garcia, A. E. True, C. J. O'Connor and J. L. Que, *Inorg. Chem.*, 1991, **30**, 1937.
41 S. Menage and J. L. Que, *Inorg. Chem.*, 1990, **29**, 4293.
42 B. Chiari, O. Piovesana, T. Tarantelli and P. F. Zanazzi, *Inorg. Chem.*, 1984, **23**, 3398.
43 S. Menage, B. A. Brennan, C. Juarez-Garcia, E. Munch and J. L. Que, *J. Am. Chem. Soc.*, 1990, **112**, 6423.
44 B. P. Murch, F. C. Bradley and J. L. Que, *J. Am. Chem. Soc.*, 1986, **108**, 5027.
45 Q. Chen, J. B. Lynch, P. Gomez-Romero, A. Ben-Hussein, G. B. Jameson, C. J. O'Connor and J. L. Que, *Inorg. Chem.*, 1988, **27**, 2673.
46 L. Ming, H. G. Jang and J. L. Que, *Inorg. Chem.*, 1992, **31**, 359.
47 B. Krebs, K. Schepers, B. Bremer, G. Henkel, E. Althaus, W. Muller-Warmuth, K. Griesar and W. Haase, *Inorg. Chem.*, 1994, **33**, 1907.
48 J. A. Bertrand and P. G. Eller, *Inorg. Chem.*, 1974, **13**, 929.
49 M. Suzuki, A. Uehara, K. Endo, M. Yanaga, S. Kida and K. Saito, *Bull. Chem. Soc. Jpn.*, 1988, **61**, 3907.

Received 29*th September* 1997; *Paper* 7/07008J